JPP JOURNAL OF PROTEINS AND PROTEOMICS
6(3), 2015, pp. 271-286

Research Article

MOLECULAR MODELING INDICATES THAT HOMOCYSTEINE INDUCES CONFORMATIONAL CHANGES IN THE STRUCTURE OF PUTATIVE TARGET PROTEINS

Yumnam Silla[1,2], Arjun Ray[1,2], Lipi Thukral[1] and Shantanu Sengupta[1,2]*

[1]*Functional Genomics Unit, CSIR-Institute of Genomics and Integrative Biology, Mathura Road, Delhi 110025, India*
[2]*Academy of Scientific and Innovative Research (AcSIR), CSIR-IGIB Campus, New Delhi, India*

Abstract: An elevated level of homocysteine, a reactive thiol containing amino acid is associated with a multitude of complex diseases. A majority (>80%) of homocysteine in circulation is bound to protein cysteine residues. Although, till date only 21 proteins have been experimentally shown to bind with homocysteine, using an *in-silico* approach we had earlier identified several potential target proteins that could bind with homocysteine. S-homocysteinylation of proteins could potentially alter the structure and/or function of the protein. Earlier studies have shown that binding of homocysteine to protein alters its function. However, the effect of homocysteine on the target protein structure has not yet been documented. In the present work, we assess conformational or structural changes if any due to protein homocysteinylation using two proteins, granzyme B (GRAB) and junctional adhesion molecule 1 (JAM1), which could potentially bind to homocysteine. We, for the first time, constructed computational models of homocysteine bound to target proteins and monitored their structural changes using explicit solvent molecular dynamic (MD) simulation. Analysis of homocysteine bound trajectories revealed higher flexibility of the active site residues and local structural perturbations compared to the unbound native structure's simulation, which could affect the stability of the protein. In addition, secondary structure analysis of homocysteine bound trajectories also revealed disappearance of â-helix within the G-helix and linker region that connects between the domain regions (as defined in the crystal structure). Our study thus captures the conformational transitions induced by homocysteine and we suggest these structural alterations might have implications for hyperhomocysteinemia induced pathologies.

Keywords: Homocysteine; disulfide; dihedral strain energy; molecular modeling; homocysteine bound target proteins.

Introduction

Homocysteine (Hcy) is a sulfur containing amino acid that is derived from methionine. It is also a key metabolite in folate mediated one carbon metabolism and transulfuration pathway. An elevated level of homocysteine (hyperhomocysteinemia) has been shown to be an independent risk factor for cardiovascular disease (Eikelboom *et al.*, 1999). Hyperhomocysteinemia is also known to be associated with a wide spectrum of complex diseases like schizophrenia (Regland *et al.*, 1995), stroke (Perry *et al.*, 1995), placental abnormalities (de Vries *et al.*, 1997), diabetes (Meigs *et al.*, 2001) and alzheimer's disease (Seshadri *et al.*, 2002) etc. Although elevated levels of homocysteine have been associated with various clinical conditions, the mechanism underlying homocysteine induced pathogenesis is not clearly understood. One of the mechanisms proposed is the "molecular targeting" hypothesis which states that homocysteine could bind to free cysteine residues

Corresponding Author: **Shantanu Sengupta**
E-mail: shantanus@igib.res.in

Received: June 3, 2015
Accepted: September 5, 2015
Published: September 7, 2015

in the protein or cleave accessible protein cysteine disulfide bonds thereby altering the structure and function of a protein (Undas *et al.*, 2001; Sengupta *et al*. 2001; Majors *et al.*, 2002; Lim *et al.*, 2003; Jacobsen *et al*., 2005). For instance, it has been shown that S-homocysteinylation of several proteins such as fibronectin, transthyretin, tissue plasminogen activator protein, factor Va, metallothionein might result in functional alteration in these proteins (Hajjar *et al.*, 1993; Undas *et al.*, 2001; Majors *et al*., 2002; Lim *et al.*, 2003; Undas *et al*., 2005; Barbato *et al.*, 2007; Colgan and Austin 2007). This hypothesis gained credence since a majority (about 70-80%) of homocysteine in circulation is found to be protein bound through disulfides (-S-S-) linkage (Mansoor *et al*., 1993; 1995; 1999; Andersson *et al*., 1995). Although several proteins could bind to homocysteine, till date only 21 proteins have been experimentally shown to bind with homocysteine (Sundaramoorthy *et al.*, 2008; Minagawa *et al.*, 2010; Tang *et al.*, 2011). Recently, we have identified several proteins that could potentially bind homocysteine based on surface accessiblilty, dihedral strain energy (DSE) of disulfide bonded cysteine or pKa of free cysteine (Silla *et al*., 2013). We speculate that binding of homocysteine with these proteins could potentially alter the local and/or global conformation of the protein.

Therefore, techniques like molecular dynamic simulations could provide better clues on how small molecules (homocysteine) affect the structure and function of biological molecules. In this study we have looked for conformational modulations if any due to protein homocysteinylation on a couple of proteins, granzyme B simulations (GRAB) and junctional adhesion molecule 1 (JAM1), identified in our previous study (Silla *et al*., 2013). Thus, to monitor structural modulation of homocysteine binding to the potential target protein, we performed molecular dynamic simulation for the wild type and homocysteine bound models and analyzed MD trajectories to ascertain the effect of homocysteine on the protein structure. In this study we for the first time developed computational simulated models for homocysteine bound proteins and have found that homocysteine added models induced conformational changes and alterations of the local secondary structure elements of the proteins which we speculate could modulate inter domain surface contact of the protein thus inhibiting interactions with the substrate or with the other proteins.

Materials and methods

Model Generation - The crystal structure of human granzyme B (PDB id: 1IAU) and JAM1 (PDB id: 1NBQ) are shown in Figure 1 and 2, respectively. Homocysteine could preferably target disulfide bonded cysteines, which have high DSE. The two disulfide bonds formed between Cys-168 and Cys-182 in granzyme B (GRAB) and Cys-153 and Cys-212 in JAM1 had highest DSE of 32.5 kJ/mol and 40.5 kJ/mol (Silla *et al*., 2013) respectively among all the disulfides present in the protein. Thus these cysteine pairs were used to generate the model structures for MD simulation. The initial atom coordinates of granzyme B and JAM1 crystal structures obtained from protein data bank (PDB id: 1IAU and 1NBQ respectively) were used to generate the starting models for the simulation as wild type (Rotonda *et al*., 2001). Using the wild type model four different models (disulfide cleaved and 3 homocysteine added models) were generated by using structure build module in Chimera (Pettersen *et al*., 2004) for both the proteins as shown in the flowchart (Figure 3). The disulfide cleaved model was built by deleting the

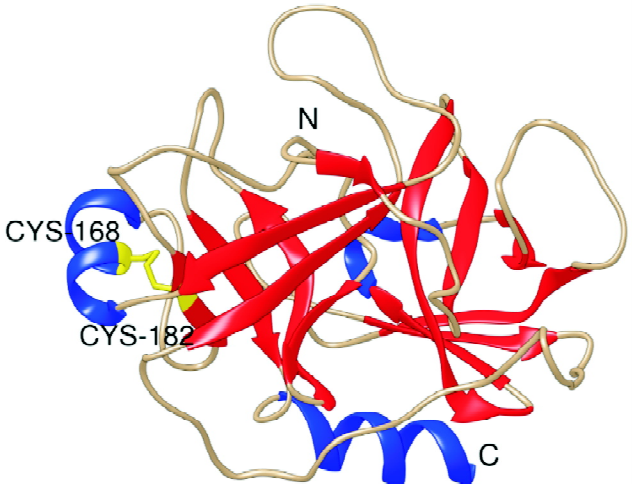

Figure 1: **Crystal structure of human granzyme B (GRAB) protein (PDB id: 1IAU). The two 6 stranded β-barrels and α-helix are shown in red and blue respectively and disulfide bonded cysteine pair used in the model generation (Cys-168-Cys-182) is represented in yellow stick**

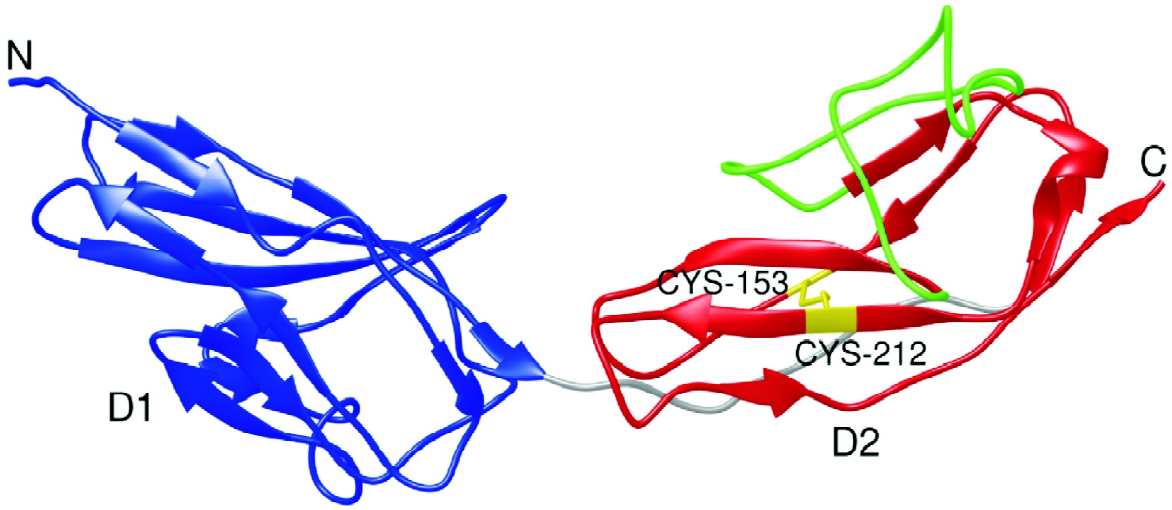

Figure 2: **Crystal structure of human junctional adhesion molecule 1 (JAM1) protein (PDB id: 1NBQ). The two domains *i.e.*, D1 and D2 are shown in blue and red respectively. The linker region between the two domains is represented in grey and the long flexible loop is shown in green. Disulfide bonded cysteine pair (Cys-153-Cys-212) in D2 domain is represented in yellow stick**

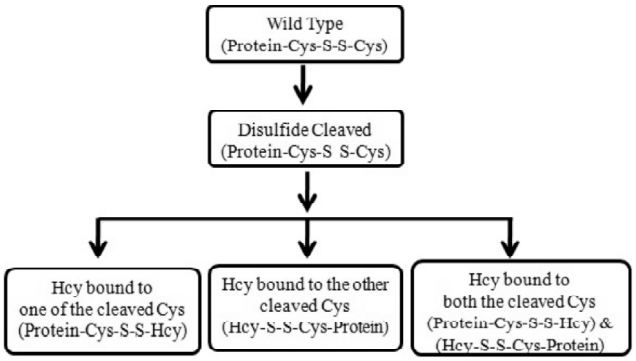

Figure 3: **Flowchart showing 5 different models: Wildtype -> disulfide bonded cysteine pair which have high DSE, Disuldife cleaved-> in which the disulfide bond formed between the cysteine pair was cleaved or deleted, Protein-Cys-S-S-Hcy -> in which Hcy was added to one of the cleaved Cys and create a disulfide bond between Cys and Hcy, Hcy-S-S-Cys-Protein -> Hcy was added to other cleaved Cys and create a disulfide bond between Cys and Hcy, Protein-Cys-S-S-Hcy & Hcy-S-S-Cys-Protein ->Hcy was added to both the cleaved cysteine**

disulfide bond (bond between the two sulfur atoms) of the cysteine pair (Cys-168 and Cys-182) in Chimera and this cleaved model was important as homocysteine first cleaved the disulfide bond when it binds to protein *via* thiol disulfide exchange reaction.

The homocysteine bound model structures were generated by creating homocysteine cysteine mixed disulfide (Hcy-S-S-Cys) bond at the disulfide cleaved cysteines [one at the Cys-168 position (Hcy-S-S-Cys-168) and the other at the Cys-182 position (Hcy-S-S-Cys-182)]. Another model that consists of two homocysteine molecules (Hcy-S-S-Cys-168&Hcy-S-S-Cys-182) was also generated. Similar exercise was employed for JAM1 and generated the five different models (Wild type, disulfide cleaved, Hcy-153, Hcy-212 and model consists of two homocysteine molecule (Hcy-153&212) using Chimera (Petterson *et al.*, 2004). All the models were subjected to energy minimization to optimize the structure using conjugate gradient algorithm. Conjugate gradient, a system developed by Magnus Hestenes and Eduard Stiefel (Magnus and Eduard, 1952), is the most widely used first derivative energy minimization method to solve an unconstrained optimization of a system.

Parameterization and addition of homocysteine-cysteine mixed disulfide (Hcy-S-S-Cys) residue to the GROMOS53 all atom force field - In this study we have used GROMOS53a6.ff all atom force field parameters to carry out MD simulation (Oostenbrink et al., 2004; Hess *et al.*, 2008). Although with recent advancement, a few MD simulation force field package have built in the capability of automatic parameter estimation for any type of molecule, however, force fields of non-standard residues may not be assigned successfully. Thus the force field parameter of homocysteine was assigned manually in order to carry out MD simulation. GROMOS53a6.ff all

atom force field file was modified by adding the new residue of homocysteine-cysteine mixed disulfide (Hcy-S-S-Cys). In order to add homocysteine residue to the force field, firstly, all atom types of Hcy-S-S-Cys was added to the ".rtp file" of GROMOS53a6.ff all atom force field, which consists of all the bonded and non-bonded information. Then all the respective files that contained the atom parameters such as hydrogen(s) database (.hdb file), atomtype(s) (atomtypes.atp) and bonded type (ffbonded.itp) information, residue database (residuetypes.dat) and special connectivity information (specbond.dat) were updated with the newly added Hcy-S-S-Cys residue type in the GROMOS53a6.ff all atom force field.

MD simulations protocol - The molecular dynamic simulation was carried out using GROMOS53a6.ff all atom force field in GROMACS version 4.5.4 (Oostenbrink *et al.*, 2004; Hess *et al.*, 2008) with explicit solvent and under periodic boundary conditions (PBC). The PBC in MD simulation is used to represent a large system in terms of a small unit cell and to simulate the solvated macromolecules in an explicit solvent environment. The starting models were neutralized with sodium ions and emerged in a periodic box of TIP3P water model that was extended to 10 Å from the solvent. The Particle Mesh Ewald method was used to treat the long-range electrostatics (Darden *et al.*, 1993) in order to improve the speed and adjust complexity during the MD simulation in a periodic system. The bond lengths within the protein were constrained using LINCS algorithm (Hess *et al.*, 1997). Energy minimization was performed using steepest descent method in order to relax the initial solvent and ion configuration and to eliminate any residual strain. To maintain the temperature of the system at a constant value of 300 K, a Berendsen thermostat (Berendsen *et al.*, 1984) was applied. The solvent and ions around the protein was equilibrated in two phase. The first phase was temperature-coupling step conducted under the NVT (constant Number of particles, Volume, and Temperature) ensemble for 0.2 ns to stabilize the temperature of the system at a constant temperature of 300K. Similarly, the second phase was pressure coupling step to equilibrate the pressure under the NPT (constant Number of particles, Pressure and Temperature) ensemble for 0.2 ns at a constant pressure of 1atm. The conformational sampling (MD simulation data collection) was started after the equilibration step at a constant pressure (1 atm) and a temperature (300K). The time steps of 0.002 ns were used to collect the MD simulation trajectory.

MD trajectory analysis - Root mean square deviation (RMSD) and root mean square fluctuation (RMSF) were calculated by using GROMACS MD analysis (g_rms and g_rmsf) tools. The RMSD is calculated as function of simulation time and computed as follows:

$$RMSD_{(t)} = \sqrt{\frac{1}{N}\sum_{i=1}^{N}(r_i(t) - r_i^{ref})^2}$$

Where N is the total number of atoms or residues included in the calculation, $r_i(t)$ is the current coordinates at time t and r_i^{ref} is the reference coordinates, computed after superimposing each frame (structure) to the reference coordinates using least square fitting. RMSD was computed for the backbone atoms and taking the starting coordinates as the reference structure. The RMSF is a measure of the flexibility of a residue. RMSF is calculated for backbone atom of each residue and it is the square root of the variance of the fluctuation around the average position. GROMACS computed RMSF as follows:

$$RMSF_{(i)} = \sqrt{\frac{1}{T}\sum_{t=1}^{T}(r_i(t) - r_i^{ref})^2}$$

Where T is the time over at which the average (r_i) and reference position (r_i^{ref}) of particle *i* is taken.

Secondary structures content - Per residue secondary structure content of each model structure as a function of simulation time was calculated using do_dssp tool implemented in the GROMACS MD simulation package. This tool uses DSSP (dictionary of secondary structure of protein) program developed by Kabsch and Sander (1983). This analysis breaks down the secondary structure information (i.e. Coil, β-Sheet, β-Bridge, bend, turn, α-Helix, 3-Helix etc.) per residue for each time step of simulation. This analysis was performed for the whole protein.

Results

The objective of the present study was to ascertain the effect of homocysteine on the structure of proteins that could potentially bind to homocysteine using molecular modeling approach. We had earlier proposed that homocysteine could bind to protein cysteine residues that are surface accessible, have high DSE (for disulfide bonded cysteine) or low pKa (for free cysteine) (Sengupta *et al.* 2001; Sundaramoorthy *et al.* 2008). DSE is a measure of the bond strength. Higher DSE indicates lower strength and hence lower stability of the disulfide bonds. Thus, disulfide bonds with higher DSE will have higher probability to be cleaved by homocysteine. Using these criteria, we have recently identified several potential protein targets that could bind with homocysteine (Silla *et al.* 2013). In the present study we have chosen two proteins (granzyme B and JAM1) that had surface accessible disulfide bonded cysteine pair with high dihedral strain energy, which we had identified as putative homocysteine target from our previous study (Silla *et al.* 2013), to evaluate if binding of homocysteine to protein cysteine results in any structural change.

Effect of homocysteine on granzyme B protein structure

Structural flexibility

The crystal structure of human granzyme B used in this study, consists of two six stranded β-barrels connected by three trans-domain segments, a long loop region and two α-helices near the C-terminal end (Figure 1). To see the effect of homocysteine on the granzyme B protein structure the disulfide bond formed between the Cys-168 and Cys-182 was used to generate the model structures. Using the wild type structure, 4 different models were developed (as shown in Figure 3) for MD simulation. These models were generated based on the different confirmations of protein bound homocyteine that exists in circulation (Sengupta *et al.*, 2001). Extensive MD simulation was carried out for 200 ns for all the models, including the wild type, by using GROMACS MD simulation package and MD trajectory were analyzed to see the structural modulation induced by homocysteine. To identify the structural flexibility induced by homocysteine on the potential target protein structure, the root mean square deviation (RMSD) and per residue root mean square fluctuation (RMSF) was calculated for each model from the MD trajectory generated during simulation.

The stability of all the models were monitored by calculating the RMSD from the starting coordinates to the end of the simulation time. The plot of RMSD of all the models as a function of simulation time is shown in Figure 4. As depicted in the figure, the RMSD of all the models increased initially due to the relaxation of the structure from the starting configuration. All the 5 models (Wild type, disulfide cleaved and 3 homocysteine added models) were stabilized during the entire simulation time as shown in Figure 4. The RMSD of the wild type is represented as black, while the disulfide cleaved model is shown in red and the 3 homocysteine added models i.e. models with Hcy-168, Hcy-182, and Hcy-168&182 are shown in green, blue and violet respectively (Figure 4).

It was interesting to see that the differences in RMSD between the simulations (except native) were subtle. We further investigated the reason why the RMSD of Hcy 168-182 final structure (200ns) was lower than the other homocysteine added structures. There was a presence of two hydrogen bonds, produced by Hcy at positions 168 and 182 holding the structure in a more compact state in the loop region of 162-179. These hydrogen bonds were missing in the other three (red, green and blue) simulations. The figure 5 illustrates this in the Hcy 168-182 200ns structure in which the loop region 162-179 is marked as pink, the key residues of 168 and 182 coloured as blue with the hydrogen bonds marked in green. The lower RMSD of Hcy 168-182 is also reflected in the increased secondary structure content compared to the other two homocysteine simulations (Table 1A).

To identify the regions of high fluctuation, the per residue root mean square fluctuation (RMSF) was calculated in all the models including the wild type as shown in Figure 6. The RMSF of the wild type granzyme B is shown in black in all the panels while the disulfide cleaved and 3 homocysteine added models are shown in red.

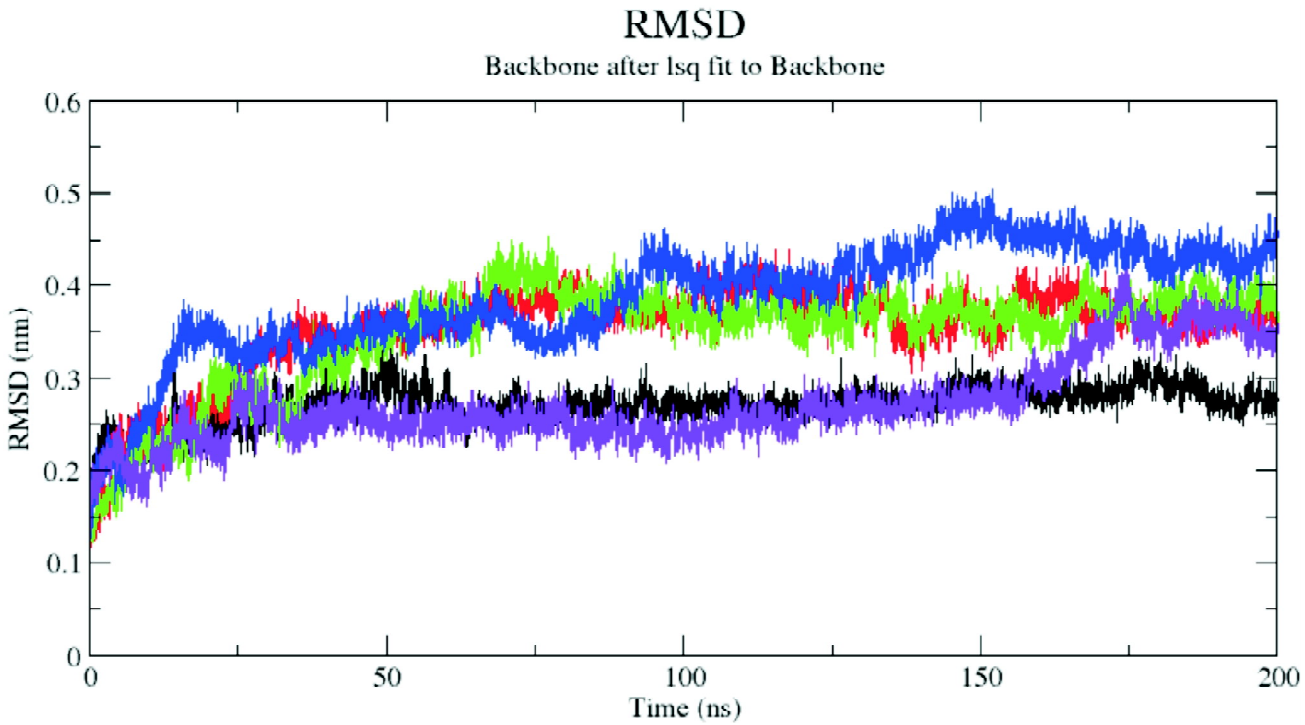

Figure 4: **Backbone RMSD plots of granzyme B protein structure showing the stability of simulation during the dynamic runs, from the starting coordinates to the end of the simulation. The models are represented as wild type in black while the cleaved model is shown in red and homocysteine added models Hcy-168, Hcy-182 and Hcy-168&182 were shown in green, blue and violet respectively**

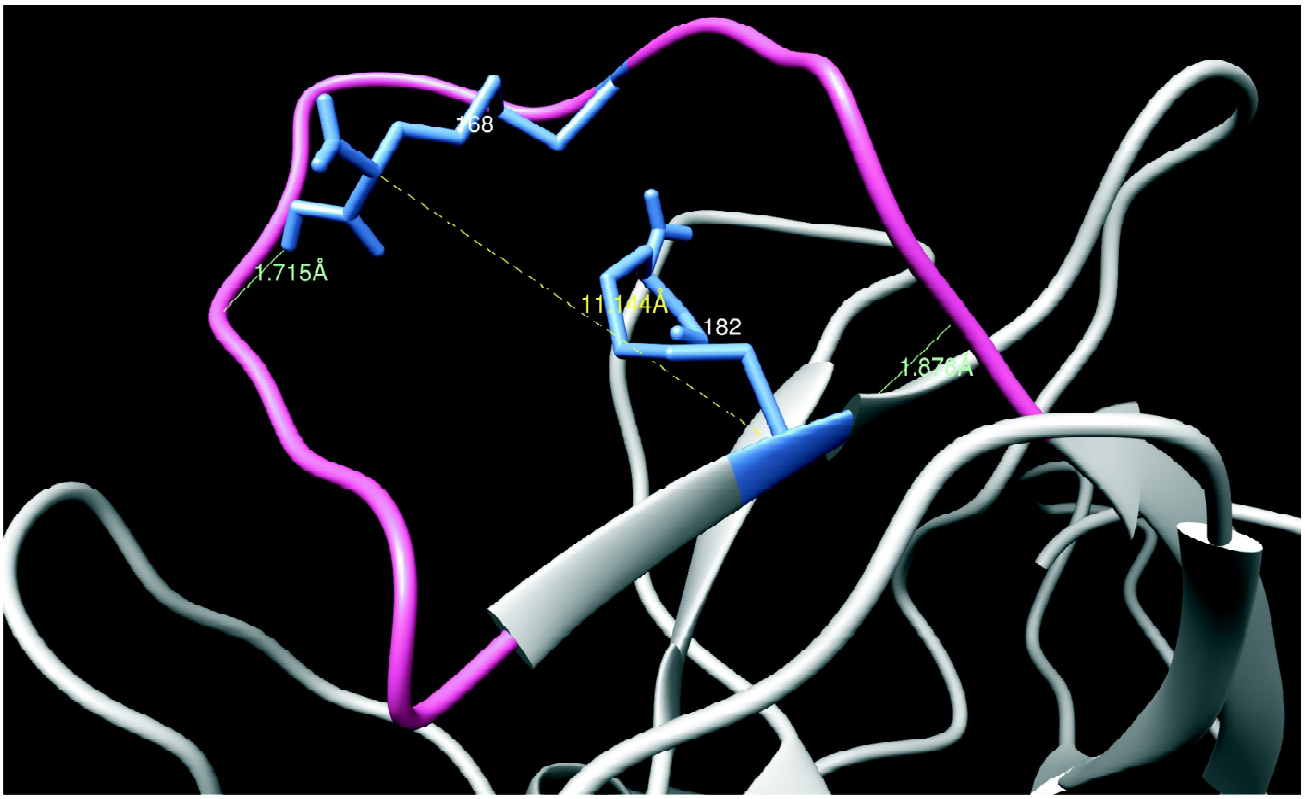

Figure 5: **Snapshot of the GRAB Hcy 168-182 200ns structure in which the loop region 162-179 is marked as pink, the key residues of 168 and 182 coloured as blue with the hydrogen bonds marked in green**

Table 1
(A) Summary of percentage of residues in different secondary structure elements (defined by DSSP) for all the models for GRAB protein's simulations. (B) Summary of percentage of residues in different secondary structure elements (defined by DSSP) for all the models for JAM1 protein

A

Secondary structure elements	*Wild Type*	*Disulphide cleaved*	*Disulphide cleaved with HCY added at residue 168*	*Disulphide cleaved with HCY added at residue 182*	*Disulphide cleaved with HCY added on 168&182*
Total	51	51	48	47	50
Coil	29	31	33	35	32
β -sheet	36	35	32	34	33
β -Bridge	2	1	3	2	3
Bend	18	18	17	16	16
Turn	11	11	11	9	10
3_{10}-Helix	2	0	1	1	1
α -Helix	3	3	2	2	3

B

Secondary structure elements	*Wild Type*	*Disulphide cleaved*	*Disulphide cleaved with HCY added at residue 153*	*Disulphide cleaved with HCY added at residue 212*	*Disulphide cleaved with HCY added on 153&212*
Total	57	60	53	56	52
Coil	26	24	31	26	31
β -sheet	48	47	44	45	41
β -Bridge	2	2	2	2	2
Bend	16	14	16	17	16
Turn	8	11	7	9	9
3_{10}-Helix	0	1	0	1	1
α -Helix	0	0	0	0	0

From the figure, it is clear that the RMSF of the N-terminal regions encompassing residue 15-130 has similar pattern of fluctuation in all the models as compared to the wild type. However, the residue encompassing 95-102 is highly fluctuated upto 0.55 nm in disulfide cleaved and Hcy added (Hcy-168 and Hcy-168&182) models (Figure 6A, B and D). This region was located at the junction of the two β-barrels that includes the active site residues Asn-95 and Asp-102, which directly interact with the tetrapeptide aldehyde inhibitor (Rotonda *et al.*, 2001). Similarly, a large fluctuation ~0.5 nm was observed at the residue encompassing 141-152 only in the wild type and disulfide cleaved models that fall in the turn regions connecting two anti-parallel β-sheets. However, this region was found to be more stable (~0.2-0.3 nm less compared to the wild type) in disulfide cleaved and homocysteine added models (Hcy-168, Hcy-182 and Hcy-168&182 model) (Figure 6B, C and D). In contrast to wild type and disulfide cleaved model, the RMSF of the homocysteine added models fluctuated differently in the C-terminal regions of the protein especially at the residues 220-230 that fluctuated upto 0.5 nm in the Hcy added models (Figure 6B, C and D). This region interestingly includes the Pro-224 and Pro-225 in the *cis* conformation. This *cis* proline conformation in human granzyme B plays a key role to orient the positively charge Arg-226 with the negatively charged group of the tetrapeptide aldehyde inhibitor (Ac-Ile-Glu-Pro-Asp-CHO) (Rotonda *et al.*, 2001).

Secondary Structure contents of granzyme B models

The changes in the secondary structure element during the simulation were calculated using DSSP (dictionary of the secondary structure of protein) analysis (Kabsch and Sander, 1983). Per residue DSSP analysis calculated over simulation time is shown in Figure 7. The percentage of residues for all the different simulated-models with different secondary structure conformation is summarized in Table 1(A).

As seen from the figure, the secondary structure elements of each model were retained over the whole MD simulation, however a few â-sheet conformations were altered into irregular secondary structure elements. Local secondary structure changes include a turn region encompassing residue 91-103 that connects two anti-parallel β-sheet was found to be transformed into a â strand that was observed for the entire simulation time in Hcy added models as compared to wild type (Figure 7, Hcy-168,Hcy-182 and Hcy168&182). Similarly, a β-sheet conformation within the residue 133-142 disappeared after 20 ns of simulation in wild type and disulfide cleaved (DC). However, this segment of the protein behaved differently in the homocysteine added models (Hcy-182, Hcy-182, Hcy-168&182) and a mixture of coil or bend structure element was observed instead of â-sheet in this region (residue 133-142) during the entire simulation. The other major structural changes include a large portion of the structure near the C-terminal region, encompassing residue 155-180. This region includes α-helix (residue 164-172) and â-sheet (residue 179-183) and both the regular secondary structure elements were transformed into a combination of coil or bend structure elements in the Hcy added (Hcy-182, Hcy-182, Hcy-168&182) model for >80% of the simulation time as shown in the Figure 7.

Effect of homocysteine on JAM 1 protein structure

The junctional adhesion molecule 1 (JAM1) protein is one of the potential homocysteine target protein. The crystal structure of the human JAM1 consists of two Ig- like domains, termed as D1 at the N-terminal and D2 at the C-terminal region (Figure 2). Each of the domains consists of one disulfide bond formed between the two opposite β-strands (Prota *et al*., 2003). The disulfide bond formed between the Cys-153 and Cys-212 has high DSE (40.1kJ/mol). Thus to see the effect of homocysteine on the JAM1 protein structure, this cysteine pair was used to generate the JAM1 model structures for MD simulation study as mentioned in the methods section. Five computational models disulfide cleaved and 3 homocysteine added models *viz* Hcy-153, Hcy-212 and Hcy-153&212 (model with 2 homocysteine molecules) models including the wild type, were generated using the starting coordinates obtained from the crystal structure and MD simulation was performed using GROMACS MD package.

Structural flexibility of JAM1 models

The stability of the models during the simulation was observed by calculating RMSD from the starting coordinates. The RMSD plots as a function of time is shown in Figure 8. The RMSD of all the models, including the wild type, increased initially up to 3Å due to the relaxation of the structure from the starting structure (Figure 8). The RMSD of the wild type (black), disulfide cleaved (red) and homocysteine added models (Hcy-153 and Hcy-153&212 represented as green and violet respectively) reached a plateau at 4 ns whereas the RMSD of the Hcy-212 model (blue) reached after 10 ns and increased up to 10 Å and retained its stability during the entire simulation time (Figure 8). The RMSD of the wild type (black), disulfide cleaved (red) and homocysteine added models (Hcy-153 and Hcy-153&212 represented as green and violet respectively) reached a plateau at 4 ns whereas the RMSD of the Hcy-212 model (blue) reached after 10 ns and increased up to 10 Å and retained its stability during the entire simulation time (Figure 8). All the simulations were carried out up to 200 ns and all the following trajectory analysis was done on the last 100 ns of the simulation where all the models reached a stable structure.

We investigated further into the reason why Hcy-212 showed a higher RMSD in comparison to other simulations. The figure 9 shows the superimposition of the 200ns structures of the

native (gold), Hcy-212 (blue) and Hcy-153&212 (pink) for the JAM1 protein's simulation. We clearly observed the right hand side domain (D2) of Hcy-212 having a distinctly different conformation compared to the other two homocysteine-added structures, which was also reflected in the high RMSD. The difference between adding one homocysteine (Hcy-212 (blue)) and two homocysteines (Hcy-153&212 (pink)) is exemplified in the figure 10. The side-chain of residue 212 was oriented towards the core of the domain. Thus, upon replacing the cysteine with homocysteine, the longer side-chain disrupted the domain. Though, contrary to intuition, adding two homocyteines actually made the domain compact again by forming hydrogen bonds between the two homocysteine residues. We also observed that D2 domain in Hcy-212 simulation was less compact compared to the other simulation. The figure 11 shows the distance between the residues 153 and 212 in the 200ns structure of the native (6.606 Å) and Hcy-212 simulation (12.039 Å). This was also accompanied with an increase in surface area for the D2 domain. There was an increase of 86 $Å^2$ in case of Hcy212 (5303 $Å^2$) in comparison to the native (5217 $Å^2$).

The regions of higher flexibility of all the models during the simulations were calculated by per residue root mean square fluctuation (RMSF) as shown in Figure 12. The RMSF of the wild type JAM 1 is shown in black in all the panels while disulfide cleaved and homocysteine added models were shown in red. The RMSF of the D1 domain (encompassing residue 25-139) at the N-terminal region of the disulfide cleaved and single homocysteine added models (Hcy-153 and Hcy-212) were found to be similar to that of wild type.

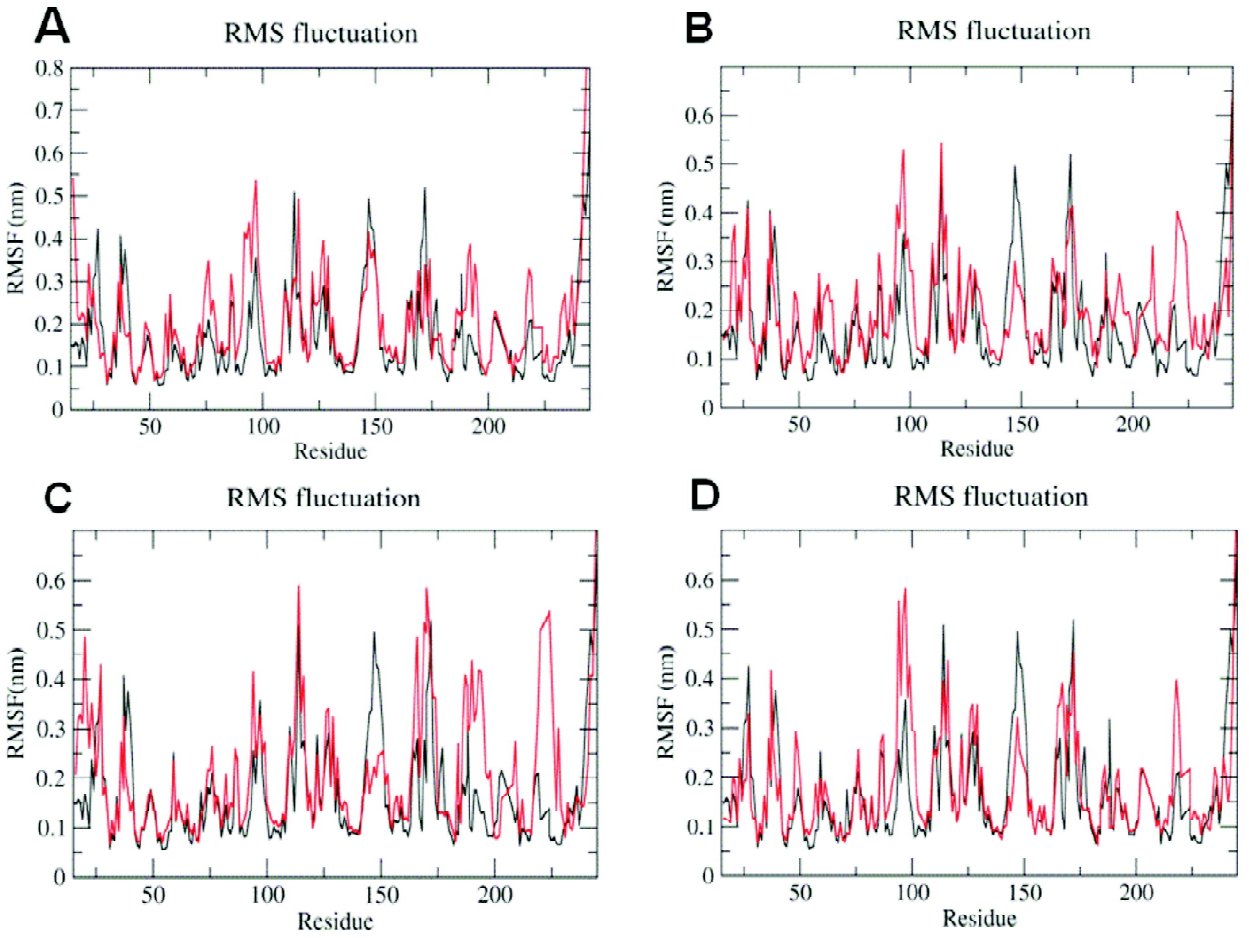

Figure 6: **Root mean square fluctuation (RMSF) of human granzyme B residues as a function of residue time, Wild type is shown in black in all the panel while the disulfide cleaved and homocysteine added models are shown in red and represented as A) disulfide cleaved B) Hcy-168, C) Hcy-182 and D) Hcy-168&182 model respectively**

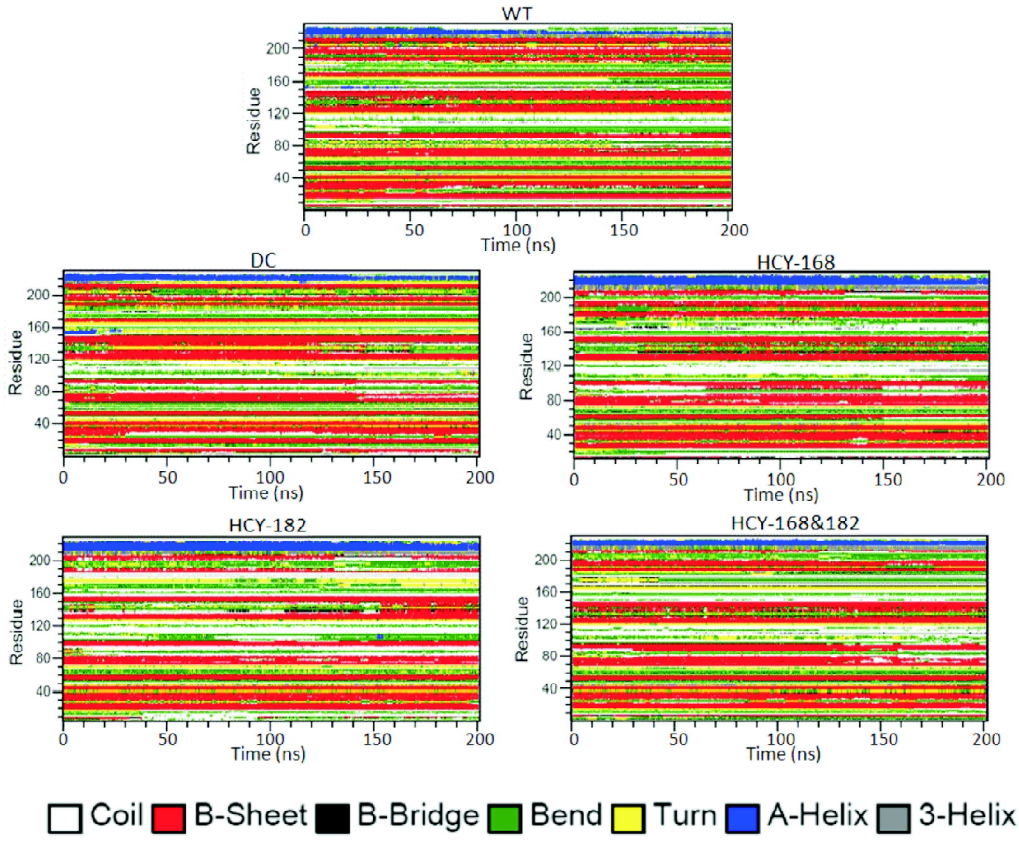

Figure 7: **Secondary structure contents of all the 5 models obtained from the dynamic trajectories. The models are represented as wild type (WT), disulfide cleaved (DC) and homocysteine added models (Hcy-168, Hcy-182 and Hcy-168&182). Each model is classified into seven secondary structures as defined by DSSP (Coil, B-sheet, B-bridge, Bend, Turn, A-Helix and 3-Helix)**

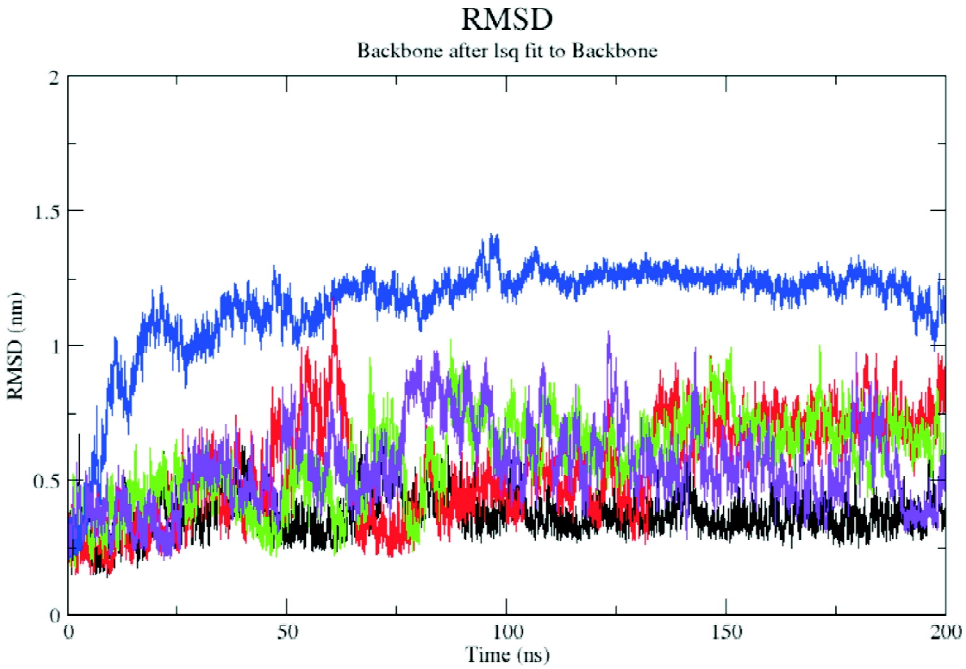

Figure 8: **Backbone RMSD plots showing the stability of simulation during the dynamic runs, from the starting coordinates to the end of the simulation. The models are represented as wild type in black while the cleaved model is shown in red and homocysteine added models Hcy-153, Hcy-212 and Hcy-153&212 were shown in green, blue and violet respectively**

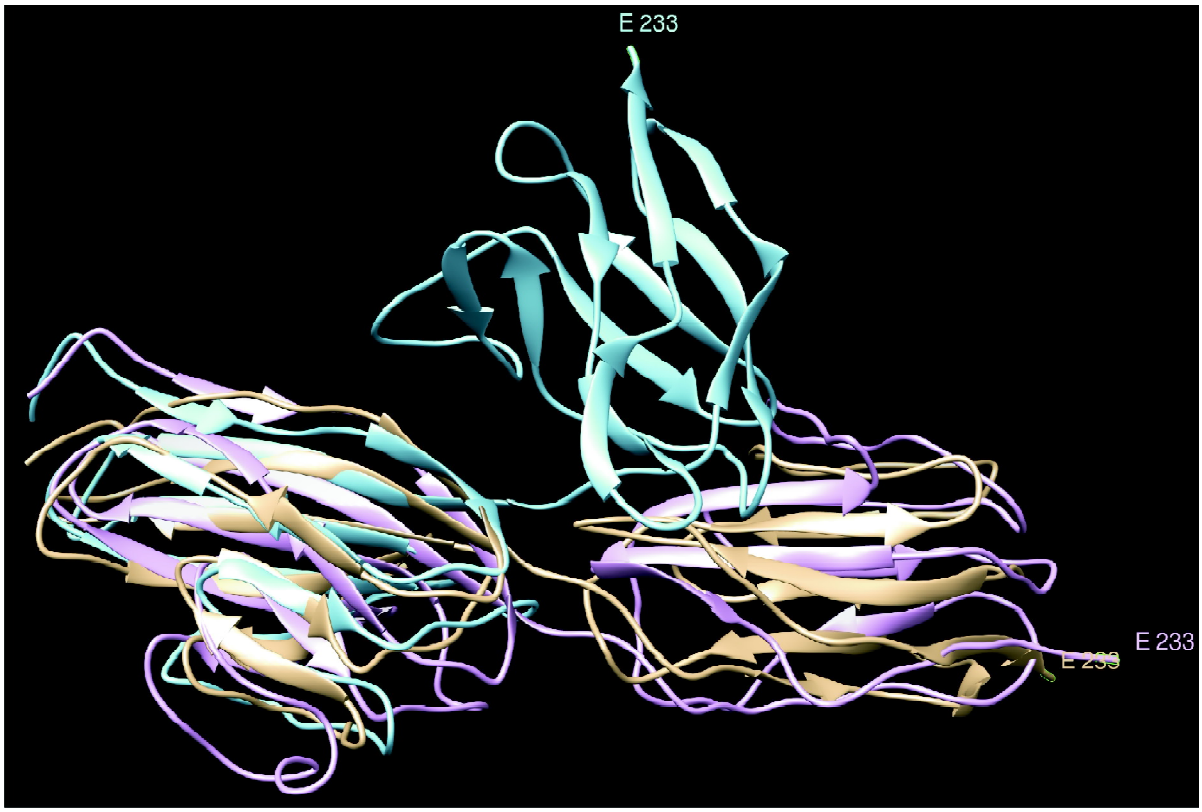

Figure 9: **Superimposition of the 200ns structures of the native (gold), Hcy212 (blue) and Hcy-153&212 (pink) for the JAM1 protein's simulation**

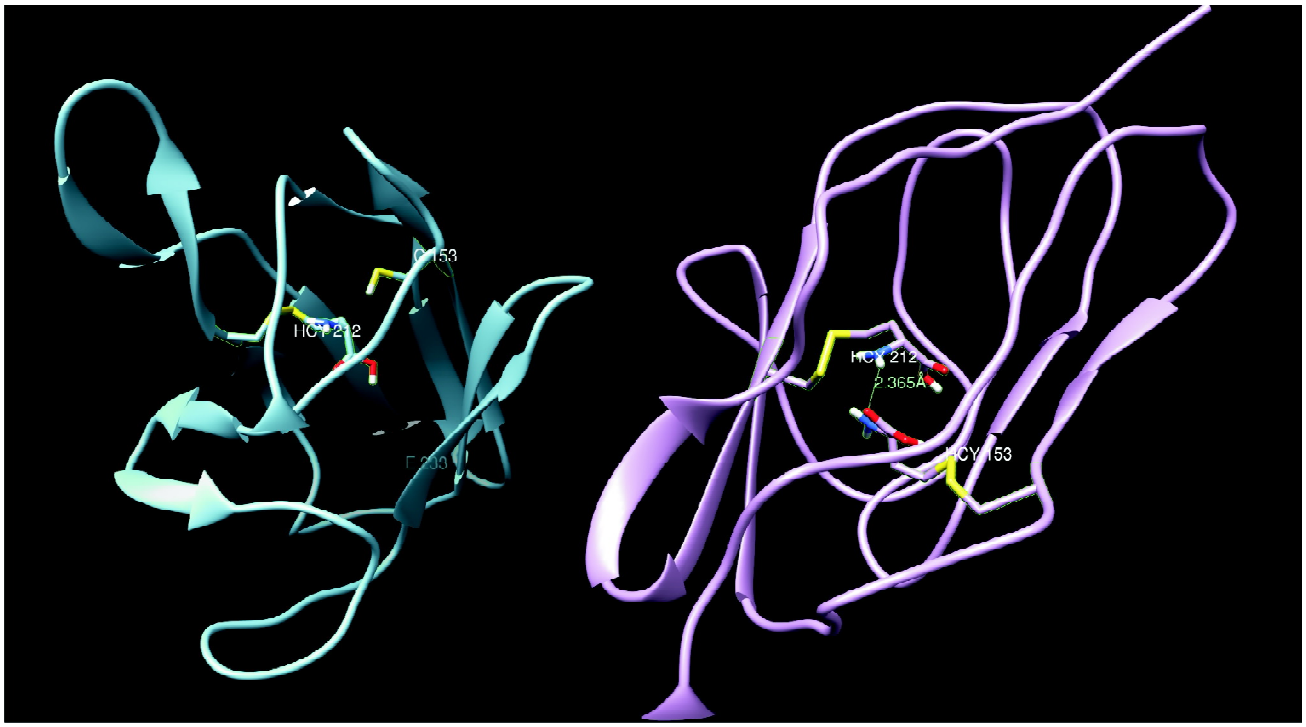

Figure 10: **Comparison between the D2 domain of JAM1 upon adding one homocysteine (Hcy212 (blue)) and two homcysteines (Hcy-153&212 (pink)). The hydrogen bond is marked in green and the residues of concern are shown in stick representation and labeled**

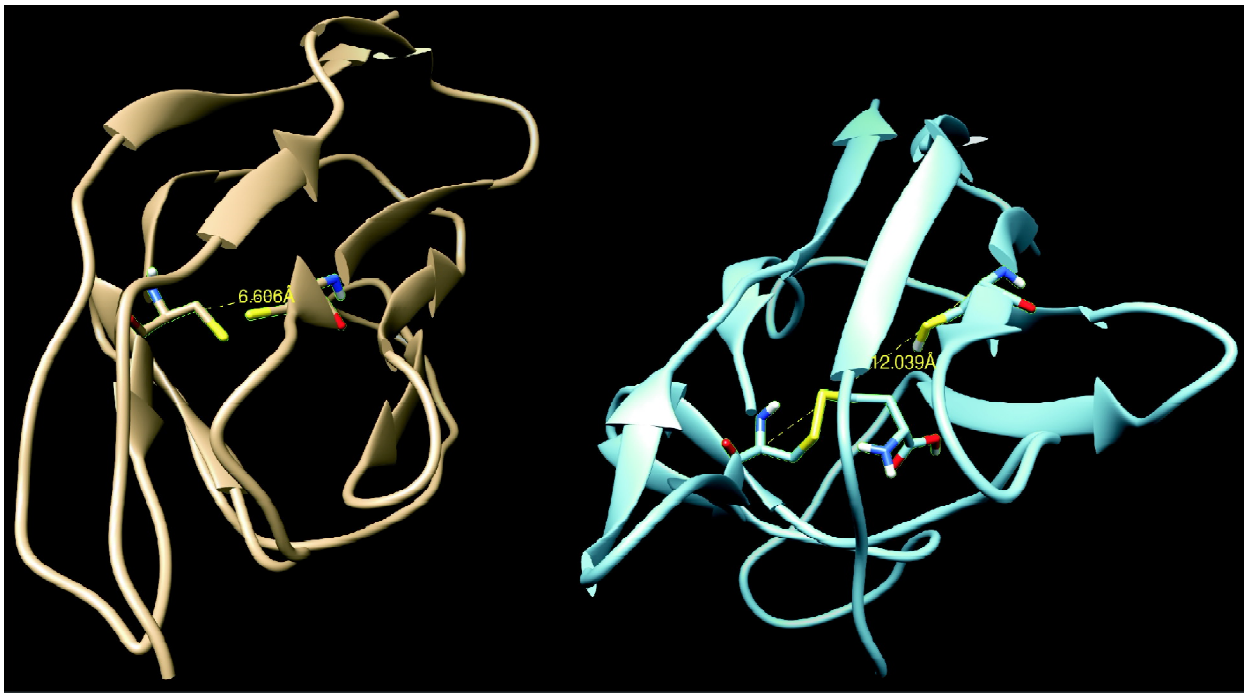

Figure 11: **Distance between the JAM1 protein's residues 153 and 212 in the 200ns structure of the native (6.606 Å) and Hcy212 simulation (12.039 Å)**

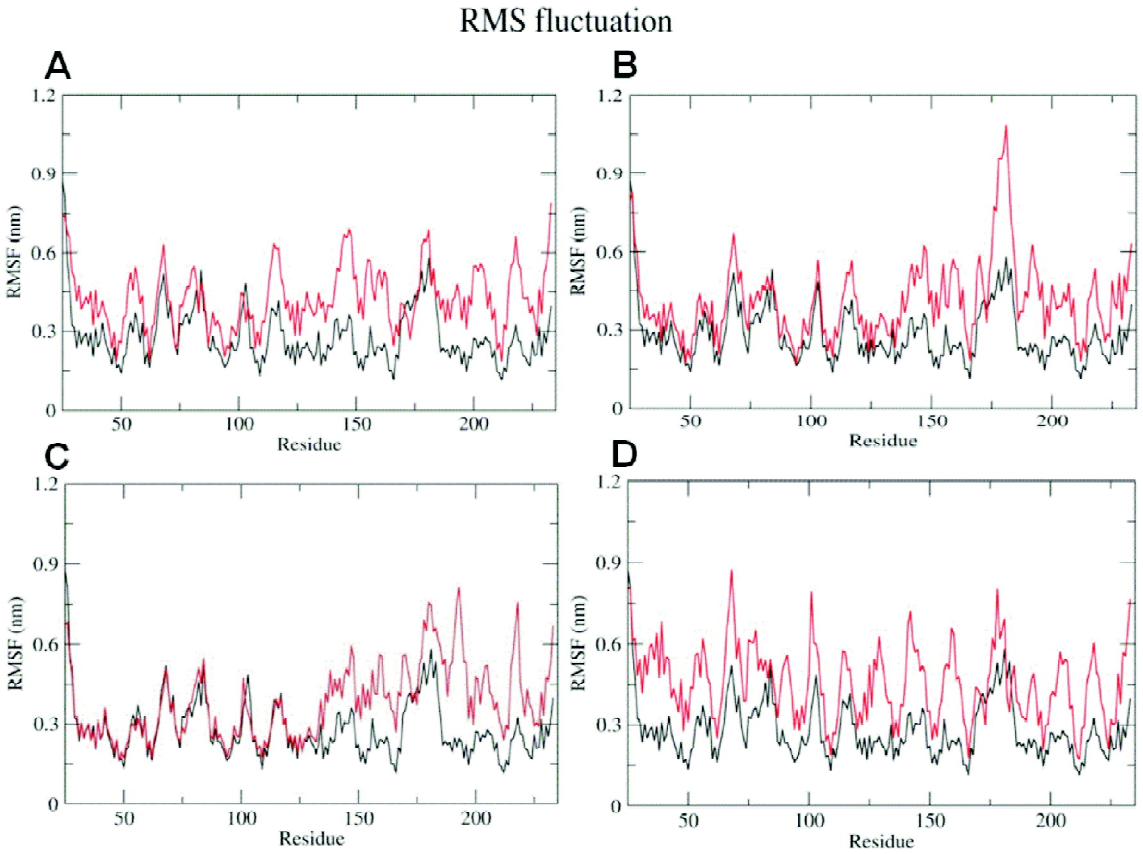

Figure 12: **Root mean square fluctuation (RMSF) of residues as a function of residue number. Wild type is shown in black. The disulfide cleaved model and homocysteine added models are shown in red and represented as A) disulfide cleaved B) Hcy-153, C) Hcy-212 and D) Hcy-153&212 models respectively**

However in the model with two homocysteine molecules (Hcy-153&212), a large fluctuation (> 0.4 nm) was observed in this region (Figure 12). Further a large fluctuation (>0.6 nm) of entire D2-domain (encompassing residue 142-233) at the C-terminal region was observed in disulfide cleaved and all homocysteine added models as compared to wild type.

Interestingly, the long flexible loop region encompassing residue 169-196 (Prota *et al*., 2003) was found to be highly fluctuating in all models, especially in Hcy-153 model (a large fluctuation (> 1 nm) was observed in this region) (Figure 12).

Secondary Structure contents of JAM1 models

The percentage of residues for all the different simulated-models with different secondary structure conformation is summarized in Table 1(B). There is a clear loss of % β-sheet when Hcy is added to either or both residues, compared to the wild type. There is also increased disorder in terms of secondary structure, which is reflected by the increase of residues in coil conformation. While there is little difference between the wild type and the disulphide cleaved model, addition of Hcy clearly induces effect on secondary structure. In Hcy-153 and Hcy-153&212 models, a complete occurrence (~99% of simulation) of coil structure in the region encompassing residue 125-138 (data not shown) that corresponds to a part of â-helix (helix G in the crystal structure) and a linker region which connects the D1 and D2 domains (Prota AE *et al*., 2003). In addition, secondary structural changes observed in these models include an extended formation of coil in D2 domain encompassing residue 148-155. This structure element was found to occur for > 60% of simulation.

Discussion

It has been reported that the molecular targeting of proteins by homocysteine via thiol disulfide exchange reaction (S-homocysteinylation) leads to the formation of stable covalent disulfide bonds with cysteine residues (Undas *et al*., 2001; Sengupta *et al*. 2001; Majors *et al*., 2002; Lim *et al*., 2003; Jacobsen *et al*., 2005). Homocysteinylation of proteins has been reported to modulate structure or functions of some proteins. For instance, binding of homocysteine with fibronectin inhibits its ability to bind fibrin (Majors *et al*., 2002). Similarly, homocysteinylation of metallothionein disrupts its ability to bind zinc and abrogates its inherent superoxide dismutase activity (Bescond *et al*., 1999). Further Hajjar (1993) and Undas *et al*., (2005) have demonstrated that homocysteine binds to tissue plasminogen activator (t-PA) and inhibits its binding to endothelial surface receptor thus promoting prothombotic state.

The structural relationship between the small molecule and its target interaction started to attract much interest in recent years. In a previous report we identified several potential target proteins that could bind with homocysteine using bioinformatics approach at a global scale (Silla *et al*., 2013). Although it is well known that S-homocysteinylation of protein cysteine residues cause protein damage by either altering the structure or function of the protein, however the effect of homocysteine on the target protein structure has not yet been documented. Thus, in the present study, conformational changes on the structure if any due to protein homocysteinylation were evaluated to understand how homocysteine binding to protein could lead to structural modulation of the target protein. For this we carried out molecular dynamic simulation of homocysteine added models of human granzyme B and JAM1 protein.

It has been reported in the crystal structure of granzyme B that majority of the active site residue Lys-192,Gly-193,Asp-194,Ser-195,Ser-214, Gly-216,Asn-218 and Arg-226 are located near the C-terminal regions (Rotonda et al., 2001) and interact with the tetra peptide aldehyde inhibitor (Ac-Ile-Glu-Pro-Asp-CHO) (Rotonda *et al*., 2001). Interestingly these regions were highly dynamic in the homocysteine added models as compared to the wild type. Further the regions encompassing 95-102 that includes active sites regions (Asn-95 and Asp-102), are also found to be more fluctuating (~0.5 nm) as compared to the wild type. Further, secondary structure analysis (DSSP) revealed alteration of a few β-sheet conformations into irregular secondary structure in the homocysteine added models. Larger fluctuation of the active site regions in the

homocysteine added models might lead to more flexibility in this region and changes of the local secondary structure elements could affect the stability of the protein structure which could inhibit the binding of inhibitor to granzyme B.

In addition, root mean square fluctuation analysis of simulated JAM1 models revealed a large fluctuation of the entire D2 domain in the disulfide cleaved and homocysteine added models, as compared to the wild type. Interestingly, in all the models, a larger fluctuation (0.3-1 nm) was observed at the long loop region (169-196) as compared to that of the wild type. This region corresponds to the long loop region at the D2 domain in the JAM1 structure data (Prota AE *et al.*, 2003). Larger fluctuation of long loop region in the models (disulfide cleaved and homocysteine added models) might lead to more flexibility in this region.

Similarly, DSSP analysis of simulated JAM1 models revealed a transformation of secondary structure elements within the structure. One of the major changes observed in the model structure, especially in Hcy-153 and Hcy-153 &212 models, was the disappearance of β-helix within the region encompassing residues 125-139 during the simulation. In the crystal structure, this region corresponds to a part of G-helix (125-131) and the linker region (134-139) respectively, that connects the D1 and D2 domains and maintained the position of the two domains in the structure (Prota *et al.*, 2003). Changes of local secondary structure element near the linker region might disturb the positioning of the domains that could modulate inter domain surface contact of the protein and thereby could inhibit the interaction of JAM1 protein to viral attachment protein ó1 during viral infection.

Conclusion

In the present study we have observed conformational changes due to binding of homocysteine (S-homocysteinylation modification) on the putative protein target's structure. This study for the first time provides MD simulation models of homocysteine with proteins. Our current analysis suggests higher flexibility of the active site residues and conformational changes of secondary structure elements into irregular structure of the homocysteine added models which could probably affect the interaction of granzyme B protein with its inhibitor. Similarly, alteration of the long loop region and local secondary structure changes in the domain region of JAM1 protein could probably affect the inter-domain surface contact of the protein that might disturb the interaction of JAM1 to the viral attachment protein σ1 during viral infection. This study suggests that S-homocysteinylation of any of the identified putative homocysteine target protein could lead us to speculate its implications for hyperhomocysteinemia induced pathologies. Further MD simulation models of homocysteine with protein would serve as a good starting platform for homocysteine modeling study in future.

Acknowledgement

Authors acknowledge grants provided by Council of Scientific and Industrial Research (CSIR), Government of India, under the project entitled "Center for Cardiovascular and Metabolic Disease Research (CARDIOMED)" (BSC0122). Authors thank Dr. Bhupesh Taneja for his valuable suggestions and the CSIR-4PI for providing the computational facility.

Abbreviations

®Hcy, homocysteine; Cys,cysteine; DSSP, dictionary of secondary structure of protein; DSE, dihedral strain energy; DC, disulfide cleave; GRAB, granzyme B; JAM1 junctional adhesion molecule 1; MD, molecular dynamic; RMSD, root mean square deviation; RMSF, root mean square fluctuation.

References

Andrea, E. P., Jacquelyn, A.C., Pierre, S., Forrest, J. C., Melissa, J. W., Timothy, R. P., Michel A. L., Beat, A. I., Terence, S. D., and Thilo, S. (2003). Crystal structure of human junctional adhesion molecule 1: Implications for reovirus binding. Proc. Natl. Acad. Sci. 100, 5366–5371.

Andersson A, Lindgren A., and Hultberg B. (1995). Effect of thiol oxidation and thiol export from erythrocytes on determination of redox status of homocysteine and other thiols in plasma from healthy subjects and patients with cerebral infarction. Clin. Chem. 41, 361-366.

Barbato JC, Catanescu O, Murray K, Dibello PM., and Jacobsen DW. (2007).Targeting of metallothionein by L-homocysteine: a novel mechanism for disruption of zinc and redox homeostasis. Arterioscler Thromb. Vasc. Biol. 27, 49–54.

Bescond A, Augier T, Chareyre C, Garcon D, Hornebeck W., and Charpiot P. (1999). Influence of homocysteine on matrix metalloproteinase-2: activation and activity. Biochem. Biophys. Res. Commun. 263, 498–503.

Berendsen, H. J. C., Postma, J. P. M., van Gunsteren, W. F., DiNola, A., and Haak, J. R. (1984). Molecular-Dynamics with Coupling to an External Bath. Journal of Chemical Physics 81, 3684–3690.

Colgan SM., and Austin RC. (2007). Homocysteinylation of metallothionein impairs intracellular redox homeostasis: the enemy within. Arterioscler Thromb. Vasc. Biol. 27, 8-11.

Darden, T., York, D., and Pedersen, L. (1993). Particle Mesh Ewald-an N. Log(N) method for Ewald sums in large systems. J. Chem. Phys. 98, 10089–10092.

de Vries, J. I., Dekker, G. A., Huijgens, P. C., Jakobs, C., Blomberg, B. M., and van Geijn HP. (1997). Hyperhomocysteinaemia and protein S deficiency in complicated pregnancies. Br. J. Obstet. Gynaecol. 104, 1248-1254.

Eikelboom, J. W., Lonn, E., Genest, J. Jr., Hankey, G., and Yusuf, S. (1999). Homocyst(e)ine and cardiovascular disease: a critical review of the epidemiologic evidence. Ann. Intern. Med. 131, 363-375

Hajjar KA. (1993). Homocysteine-induced modulation of tissue plasminogen activator binding to its endothelial cell membrane receptor. J. Clin Invest. 91, 2873–2879.

Hestenes, Magnus R., and Stiefel, Eduard (1952). Methods of Conjugate Gradients for Solving Linear Systems. Journal of Research of the National Bureau of Standards 49, 409-436.

Hess, B., Bekker, H., Berendsen, H.J.C., Fraaije., and J.G.E.M. (1997). LINCS: A linear constraint solver for molecular simulations. J. Comput. Chem. 18, 1463–1472.

Hess, B., Kutzner, C., Spoel, D., and Lindahl, E. (2008). GROMACS 4: Algorithms for Highly Eûcient, LoadBalanced, and Scalable Molecular Simulation. J. Chem. Theory Comput. 4, 435–447.

Hubmacher, D., Tiedemann, K., Bartels, R., Brinckmann, J., and Vollbrandt, T. (2005). Modification of the structure and function of fibrillin-1 by homocysteine suggests a potential pathogenetic mechanism in homocystinuria. J. Biol. Chem. 280, 34946-34955.

Jacobsen, D. W., Catanescu, O., Dibello, P. M., and Barbato, J. C. (2005). Molecular targeting by homocysteine: a mechanism for vascular pathogenesis. Clin. Chem. Lab. Med. *43,* 1076-1083.

Kabsch, W., and Sander, C. (1983). Dictionary of protein secondary structure: pattern recognition of hydrogen-bonded and geometrical features. Biopolymers 22, 2577-2537.

Lim, A., Sengupta, S., McComb, M. E., Théberge, R., Wilson, W. G., Costello, C. E., and Jacobsen, D. W. (2003). In vitro and in vivo interactions of homocysteine with human plasma transthyretin. J. Biol. Chem. 278, 49707-49713.

Majors, A.K., Sengupta, S., Willard, B., Kinter, M. T., and Pyeritz, R. E. (2002). Homocysteine binds to human plasma fibronectin and inhibits its interaction with fibrin. Arterioscler. Thromb. Vasc. Biol. 22, 1354-1359.

Mansoor, M. A., Bergmark, C., Svardal, A. M., Lønning, P. E., and Ueland, P. M. (1995). Redox status and protein binding of plasma homocysteine and other aminothiols in patients with early-onset peripheral vascular disease. Homocysteine and peripheral vascular disease. Arterioscler Thromb. Vasc. Biol. 15,232-240.

Mansoor, M. A., Kristensen, O., Hervig, T., Bates, C. J., Pentieva, K., Vefring, H., Osland, A., Berge, T., Drabløs, P. A., Hetland, O., and Rolfsen, S. (1999). Plasma total homocysteine response to oral doses of folic acid and pyridoxine hydrochloride (vitamin B_6) in healthy individuals. Oral doses of vitamin B6 reduce concentrations of serum folate. Scand. J. Clin. Lab. Invest. 59, 139-146.

Mansoor, M. A., Svardal, A. M., and Ueland, P. M. (1992). Determination of the in vivo redox status of cysteine, cysteinylglycine, homocysteine, and glutathione in human plasma. Anal. Biochem. 200, 218-229.

Mansoor, M. A., Ueland, P. M., Aarsland, A., and Svardal, A. M. (1993). Redox status and protein binding of plasma homocysteine and other aminothiols in patients with homocystinuria. Metabolism 42, 1481–1485.

Meigs, J. B., Jacques, P. F., Selhub, J., Singer, D. E., and Nathan, D. M. (2001). Fasting plasma homocysteine levels in the insulin resistance syndrome: the Framingham offspring study. Diabetes Care 24, 1403-1410.

Mills, J. L., McPartlin, J. M., Kirke, P. N., Lee, Y. J., Conley, M. R., Weir, D. G., and Scott, J. M. (1995). Homocysteine metabolism in pregnancies complicated by neural-tube defects. Lancet 345, 149-151

Minagawa H., Watanabe A., Akatsu H., Adachi K., and Ohtsuka C. (2010). Homocysteine, another risk factor for Alzheimer disease, impairs apolipoprotein E3 function. J. Biol. Chem. 285, 38382-38388.

Oostenbrink C., Villa, A., Mark, A. E., and van Gunsteren, W. (2004). A biomolecular force field based on the free enthalpy of hydration and solvation: the GROMOS force-field parameter sets 53A5 and 53A6. Journal of Computational Chemistry 25, 1656–1676.

Perry, I. J., Refsum, H., Morris, R. W., Ebrahim, S. B., and Ueland, P. M. (1995). Prospective study of serum total homocysteine concentration and risk of stroke in middle-aged British men. Lancet 346, 1395-1398.

Pettersen, E. F., Goddard, T. D., Huang, C. C., Couch, G. S., Greenblatt, D. M., Meng, E. C., and Ferrin, T. E. (2004). UCSF chimera; a visualization system for exploratory research and analysis. J. Comput. Chem. 25, 1605–1612.

Prota A.E., Campbell J.A., Schelling P., Forrest J.C., Watson M.J., Peters T.R., Aurrand-Lions M., Imhof B.A., Dermody T.S., and Stehle T. (2003). Crystal structure of human junctional adhesion molecule 1: implications for reovirus binding. Proc. Natl. Acad. Sci. 29, 5366-5371.

Regland, B., Johansson, B. V., Grenfeldt, B., Hjelmgren, L. T., and Medhus, M. (1995). Homocysteinemia is a common feature of schizophrenia. J. Neural Transm. Gen. Sect. 100, 165-169.

Rotonda J., Garcia-Calvo M., Bull H.G., Geissler W.M., McKeever B.M., Willoughby C.A., Thornberry N.A., and Becker J.W. (2001). The three-dimensional structure of human granzyme B compared to caspase-3, key mediators of cell death with cleavage specificity for aspartic acid in P1. Chem. Biol. 8,357-368.

Sengupta, S., Chen, H., Togawa, T., DiBello, P. M., Majors, A. K. Büdy, B., Ketterer, M. E., and Jacobsen, D. W. (2001). Albumin thiolate anion is an intermediate in the formation of albumin-S-S-homocysteine. J. Biol. Chem. 276, 30111-30117.

Sengupta, S., Wehbe, C., Majors, A. K., Ketterer, M. E., and DiBello, P. M. *et al.* (2001). Relative roles of albumin and ceruloplasmin in the formation of homocystine, homocysteine-cysteine-mixed disulfide, and cystine in circulation. J. Biol. Chem. 276, 46896-46904.

Seshadri, S., Beiser, A., Selhub, J., Jacques, P. F., and Rosenberg, I. H. *et al.* (2002). Plasma homocysteine as a risk factor for dementia and Alzheimer's disease. N. Engl. J. Med. 346, 476-483.

Silla, Y., Sundaramoorthy, E., Talwar, P., and Sengupta, S. (2013). S-linked protein homocysteinylation: identifying targets based on structural, physicochemical and protein-protein interactions of homocysteinylated proteins. Amino Acids 44, 1307-1316.

Sundaramoorthy, E., Maiti, S., Brahmachari, S. K., and Sengupta, S. (2008). Predicting protein homocysteinylation targets based on dihedral strain energy and pKa of cysteines. Proteins 71, 1475-1543.

Tang Y.S., Khan R.A., Zhang Y., Xiao S., and Wang M. (2011). Incrimination of heterogeneous nuclear ribonucleoprotein E1 (hnRNP-E1) as a candidate sensor of physiological folate deficiency. J. Biol. Chem. 286, 39100-39115.

Undas, A., Brozek, J., and Szczeklik, A. (2005). Homocysteine and thrombosis: from basic science to clinical evidence. Thromb. Haemost. 94, 907-915.

Undas, A., Williams, E. B., Butenas, S., Orfeo, T., and Mann, K. G. (2001). Homocysteine inhibits inactivation of factor Va by activated protein C. J. Biol. Chem. 276, 4389-4397.